Excited State Dynamics of Organo-Lanthanide Electroluminescent Phosphors: The Properties of Tb(tb-pmp)$_3$ and Gd(tb-pmp)$_3$

J. R. G. Thorne,* J. M. Rey, R. G. Denning, S. E. Watkins, M. Etchells, M. Green, and V. Christou

Department of Chemistry, University of Oxford, Inorganic Chemistry Laboratory South Parks Road, Oxford, OX1 3QR, United Kingdom

Received: October 25, 2001; In Final Form: February 7, 2002

The excitation energy transfer rates between the excited states of a Tb(III) complex containing the ligand 1-phenyl-3-methyl-4-(trimethylacetyl)pyrazol-4-one, are described. Energy transfer rate constants are derived from time-gated and time-correlated single photon counting measurements. Comparison with the analogous Gd(III) complex shows that there is efficient intramolecular energy transfer from a singlet state of the ligand to excited terbium *f*-electron states. There is no evidence of bi-exciton annihilation in these materials, even at very high exciton densities. The use of this complex as the active medium for electroluminescent device applications is addressed. We note the particular properties of the ligand which make it suitable for this application and suggest possible improvements.

1. Introduction

Molecular lanthanide complexes show promising properties as phosphors in thin film organic electroluminescent displays.[1−7] The narrow lanthanide emission bands offer superior spectral purity, whereas the chemical flexibility of the complexes provides a platform for manipulating the physical properties of the emitter.[8] Up to now, complexes containing β-diketonate ligands have attracted much attention,[9−12] but other ligands have also been investigated.[7,13]

Recently, a high efficiency green electroluminescent device based on an organo-terbium complex has been reported.[13] This complex contains three 1-phenyl-3-methyl-4-(trimethylacetyl)-pyrazol-4-one (tb-pmp, **I**) ligands. Because the performance of an organolanthanide-based light emitting diode (OLED) depends on the efficiency of the transfer of excitation energy to the lanthanide ion, we have sought to understand the relevant photophysical properties of these *tb-pmp* based OLED materials. Here, we present the results of a study of the Gd(tb-pmp)$_3$ and Tb(tb-pmp)$_3$ complexes.

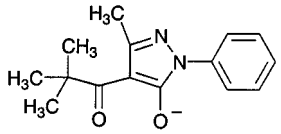

I

tb-pmp

In Gd(tb-pmp)$_3$, excited states derived from the f^7 configuration of the Gd^{3+} ion lie above 4 eV, and also well above those associated with the lowest energy ligand-based excitations near 2.6 eV. The observed luminescence, following internal relaxation, is entirely attributable to ligand-based transitions. Given that the bonding in lanthanide complexes is primarily ionic in character,[14] and that the ionic radius of Gd^{3+} (93.8 pm) is very close to that of Tb^{3+} (92.3 pm),[15] it is safe to assume that the electronic structure of the ligands is effectively the same in Gd(tb-pmp)$_3$ and Tb(tb-pmp)$_3$. With this in mind, we make the assumption throughout this work that ligand-based photophysical processes should be comparable in both compounds.

In organo-lanthanide complexes of this type, the energy transfer route from a ligand-centered excitation to metal-localized one, has generally been interpreted as a two-step process, involving initially ligand singlet-to-triplet inter-system crossing, followed by ligand triplet-to-metal excitation transfer (e.g., Buono-Core[16] and references therein). In this paper, we examine the validity of this mechanism by means of the optical measurement of the excited-state dynamics.

2. Experimental Section

2.1. Synthesis. The pyrazolone ligands were synthesized using conventional techniques.[17] Initially complexes with the composition Tb(tb-pmp)$_3$.$Ph_3PO{\cdot}H_2O$, were synthesized.[18] The fabrication of electroluminescent devices requires the vapor phase deposition of thin films of the complexes. However during the evaporation, the Ph_3PO coligand partially dissociates, yielding films whose Ph_3PO content is variable and nonstoichiometric. To solve this problem, we have developed a route to the homoleptic Gd(tb-pmp)$_3$ and Tb(tb-pmp)$_3$ complexes, as described below. Mixed materials, in which either 1 mol % or 5 mol % of the gadolinium complex was replaced by the terbium analogue were also prepared to yield a solid solution as indicated below.

All these materials contain no coligands, are stoichiometric, and of high purity. As evaporated, they form thin glassy films. They have well-defined and reproducible excitation dynamics. On the other hand the reproducibility of EL devices made from nonstoichiometric precursors was very variable. Photoluminescence lifetime measurements on the evaporated nonstoichiometric materials showed a complex time-dependence that could not be fitted to a single-exponential decay.[18]

Synthesis of 1-phenyl-3-methyl-4-(2,2-dimethylpropan-1-oyl)pyrazolin-5-one (Bu^{t}pmp). A mixture of 1-phenyl-3-

* To whom correspondence should be addressed. E-mail: jonathan.thorne@chem.ox.ac.uk.

10.1021/jp013955s CCC: $22.00
Published on Web 03/30/2002

methylpyrazolin-5-one (24 g, 0.14 mol) and 1,4-dioxane (600 mL) in a 1 L flask equipped with a mechanical stirrer was heated at 70 °C for 10 min. To the resulting yellow solution was added calcium hydroxide (30 g, 0.52 mol) in small portions over a 10 min period. The resulting pink colored mixture was allowed to cool to room temperature and then trimethylacetyl chloride (21 g, 0.17 mol) was added dropwise. The resulting mixture was heated to reflux whereupon the mixture became paler and considerably more viscous. The reaction was maintained at reflux for a further 18 h. The cloudy pinkish mixture was cooled to room temperature and poured into a stirred solution of ice cold hydrochloric acid (1.2 L of a 3 M solution). The mixture immediately changed color to pale brown, became cloudy and effervesced. Within 90 min a significant amount of solid had begun to precipitate and the solution became clearer. Stirring was continued for a further 15 h. The pink/brown precipitate was isolated by vacuum filtration and dried under vacuum to give 11.0 g of a tan solid. Sublimation (95 °C, $\sim 10^{-6}$ mbar) of this product gave analytically pure product as a pale yellow solid (4.6 g, 17.8 mmol, 13%). mp 91−92 °C; δ_H (500 MHz; $CDCl_3$) 14.92 (1 H, s, pyrazolone), 7.86 (2 H, d, *J* 8 Hz, 2′,6′-H), 7.48 (2 H, t, *J* 7.5 Hz, 3′,5′-H), 7.32 (1 H, t, *J* 7.5 Hz, 4′-H), 2.65 (3 H, s, Me), 1.41 (9 H, s, *tert*-Bu). Anal. Calcd. for $C_{15}H_{18}N_2O_2$: C, 69.8; H, 7.02; N, 10.8. Found: C, 69.7; H, 7.04; N, 10.8.

Synthesis of [Tb(Bu^{t}pmp)$_3$(bpy)]. A mixture of Bu^{t}pmp (2.1 g, 8.1 mmol), sodium hydroxide (0.32 g, 8.0 mmol) and 2,2′-bipyridine (0.42 g, 2.7 mmol) in ethanol (90 mL) and water (90 mL) was stirred for 1 h whereupon the solids had completely dissolved. This solution was then treated with a solution of $TbCl_3 \cdot 6H_2O$ (1.0 g, 2.7 mmol) in water (10 mL) which resulted in the immediate formation of a white precipitate. Stirring was continued for 1.5 h. The colorless precipitate was then collected by vacuum filtration, washed with water (50 mL) and dried under vacuum to give the product as a colorless solid (2.80 g, 90%). Anal. Calcd for $C_{55}H_{59}N_8O_6Tb \cdot H_2O$: C, 59.8; H, 5.56; N, 10.1; Tb, 14.4. Found: C, 59.4; H, 5.17; N, 10.3; Tb, 14.7.

Synthesis of [Tb(Bu^{t}pmp)$_3$]. [Tb(Bu^{t}pmp)$_3$(bpy)] (2.6 g, 2.3 mmol) was heated at 200 °C under vacuum (1×10^{-7} mbar) for 1.5 h. When all of the 2,2′-bipyridine had evolved the temperature was increased to 300 °C, and the complex was sublimed over 5 h. The purified material was resublimed (300 °C, 1×10^{-7} mbar) to give the homoleptic complex as a colorless sublimate (1.4 g, 1.5 mmol, 65%). Anal. Calcd for $C_{45}H_{51}N_6O_6Tb$: C, 58.1; H, 5.52; N, 9.03; Tb, 17.1. Found: C, 58.5; H, 5.34; N, 9.21; Tb, 17.1.

Synthesis of [Gd(Bu^{t}pmp)$_3$(bpy)]. A mixture of Bu^{t}pmp (2.3 g, 8.8 mmol), sodium hydroxide (0.35 g, 8.8 mmol) and 2,2′-bipyridine (0.46 g, 2.9 mmol) in ethanol (100 mL) and water (100 mL) was stirred for 1 h, whereupon the solids had completely dissolved. This solution was then treated with a solution of $GdCl_3 \cdot 6H_2O$ (1.1 g, 2.9 mmol) in water (15 mL) which resulted in the immediate formation of a white precipitate. Stirring was continued for 1 h. The white precipitate was then collected by vacuum filtration, washed with water (50 mL) and dried under vacuum, to give the product as a colorless solid (2.3 g, 72%). Anal. Calcd for $C_{55}H_{59}N_8O_6Gd \cdot H_2O$: C, 59.9; H, 5.57; N, 10.2; Gd, 14.3. Found: C, 59.7; H, 5.67; N, 10.3; Gd, 14.3.

Synthesis of [Gd(Bu^{t}pmp)$_3$]. [Gd(Bu^{t}pmp)$_3$(bpy)] (0.84 g, 0.72 mmol) was heated at 200 °C under vacuum (1×10^{-7} mbar) for 1 h, by which time all of the 2,2′-bipyridine had evolved. The temperature was increased to 300 °C, and the complex was sublimed over 5 h. The purified material was resublimed (300 °C, 1×10^{-7} mbar) to give the homoleptic complex as a colorless sublimate (0.57 g, 0.61 mmol, 85%). Anal. Calcd for $C_{45}H_{51}N_6O_6Gd$: C, 58.2; H, 5.53; N, 9.04; Gd, 16.9. Found: C, 58.2; H, 5.54; N, 9.02; Gd, 17.0.

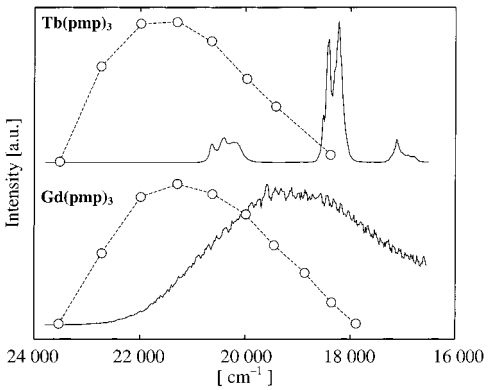

Figure 1. Fluorescence spectra (- -o- -) of Tb(tb-pmp)$_3$ and Gd(tb-pmp)$_3$ obtained by integrating emission during the first 400ps after the laser pulse at 27 780 cm^{-1}. Full lines present Tb(tb-pmp)$_3$ metal emission spectrum (1 ms gate delayed by 0.5 ms) and phosphorescence emission spectrum of Gd(tb-pmp)$_3$ (1 ms gate delayed by 30 μs) at 295 K after excitation at 28 170 cm^{-1}.

Synthesis of 1 mol % [Tb(Bu^{t}pmp)$_3$] in [Gd(Bu^{t}pmp)$_3$]. [Tb(Bu^{t}pmp)$_3$(bpy)] (0.011 g, 0.012 mmol) and [Gd(Bu^{t}pmp)$_3$-(bpy)] (1.09 g, 1.17 mmol) were dissolved in dichloromethane (3 mL) and the solution transferred to a sublimation tube. The solvent was removed under vacuum and the mixed solid twice sublimed under vacuum (300 °C, 1×10^{-7} mbar). The resulting sublimate was transferred into a quartz tube in a nitrogen filled glovebox and sealed under vacuum.

2.2. Optical Measurements. Fluorescence decays were obtained by time-correlated single-photon counting (TCSPC), following excitation by a frequency-doubled mode-locked Ti: sapphire laser (Tsunami, Spectra-Physics 150 fs) operating at 27 780 cm^{-1} (360 nm) with a pulse repetition rate of 80 MHz. The detection system consisted of a monochromator (H10, Jobin-Yvon) followed by a microchannel-plate (R3809U, Hamamatsu). A combination of color and interference filters were used to remove scattered laser light. The instrument response function, obtained from the sample scattering detected near the laser wavelength, had a fwhm of 38 ps. Lifetimes were obtained by fitting the convolutions of the instrument function with the experimental decays.

Time-resolved measurements on the nanosecond to microsecond time scale were performed by excitation with the third harmonic (28 170 cm^{-1}, 355 nm) of a pulsed Nd:YAG laser (SL803, Spectron). The repetition rate was 10 Hz and the pulse width 8 ns. The emission was analyzed with a monochromator (Spex 1404) and detected with a photomultiplier (EMI 9813QB), followed either by a photon-counting unit (SR400, Stanford Research), a boxcar averager (SR250, Stanford Research) or a digital oscilloscope (Hewlett-Packard 54111D).

3. Results

3.1. Fluorescence. The fluorescence spectra of Gd(tb-pmp)$_3$ and Tb(tb-pmp)$_3$ were obtained by integrating the TCSPC emission during the first 400 ps after the Ti:sapphire laser excitation pulse. They consist of a broad feature (fwhm 3500 cm^{-1}) with a maximum near 21 400 cm^{-1} (Figure 1). Both spectra have their maxima at the same energy and have similar spectral bandwidths.

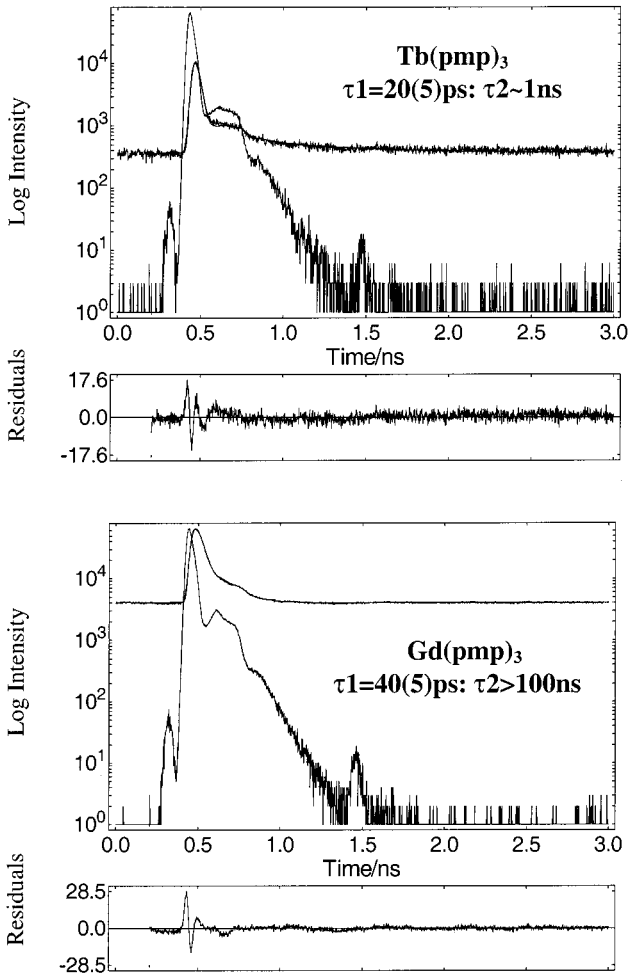

Figure 2. Picosecond kinetics. Fluorescence decays excited at 27 800 cm^{-1} and detected at 21 300 cm^{-1} of Tb(tb-pmp)$_3$ and Gd(tb-pmp)$_3$ at room temperature. The upper traces represent the observed decays and the lower ones the corresponding instrument functions. The decays are fitted with a convolution of the instrument function with a double exponential.

The decay of the fluorescence was fitted by a convolution of the instrumental function with either a single or double exponential (Figure 2). In Gd(tb-pmp)$_3$, both the single-exponential fit, and the dominant short-lived component of the double exponential fit, have a characteristic (1/e) decay time of 40(5) ps. This lifetime is independent of the detection wavelength, in the range 23 500−19 400 cm^{-1}. It is clear from Figure 2 that there is also a long-lived background emission, from both materials. This is strong (i.e., 300−4000 c/s) compared to the instrumental background (∼3 c/s). It is due to a phosphorescence signal whose decay time is long compared to the interval between successive laser pulses (12.5 ns). There is a small (∼1%) contribution to the emission having a lifetime of a few nanoseconds, that may arise from impurity fluorescence. Its inclusion in a double exponential model, improves the fit to the dominant short-time component in Figure 2. Using the same procedure, the fluorescence decay of Tb(tb-pmp)$_3$ can also be fitted to a double exponential; the dominant fast contribution in this case has a characteristic decay time of 20(5) ps (Figure 2) at all detection wavelengths in the above range.

3.2. Phosphorescence. The phosphorescence spectrum of Gd-(tb-pmp)$_3$, recorded with a 1ms gate delayed by 30 μs relative to the laser pulse, shows a maximum at 19 200 cm^{-1} and a fwhm of 3800 cm^{-1} (Figure 1).

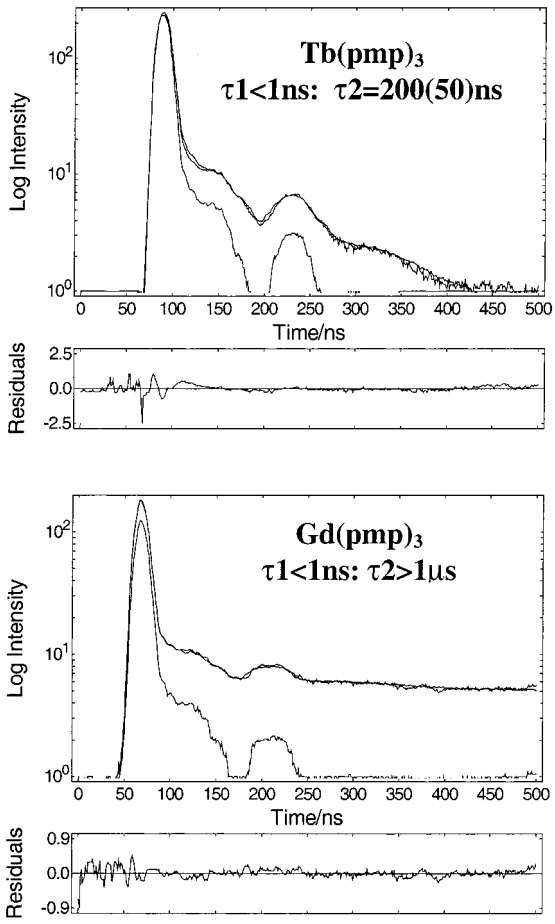

Figure 3. Nanosecond kinetics. Phosphorescence decay of Tb(tb-pmp)$_3$ and Gd(tb-pmp)$_3$ at room temperature, detected at 19 200 cm^{-1} after excitation at 28 170 cm^{-1}. Upper traces lines represent observed decays and lower ones the corresponding instrument functions (fluorescence detected at 21 300 cm^{-1}). The decays are fitted with a convolution of the instrument function with a double exponential.

The decay of the phosphorescence was fitted by a convolution of the instrumental function (8 ns laser pulse) with a double exponential (Figure 3). In Gd(tb-pmp)$_3$, the phosphorescence does not decay on a 500 ns time scale, and residual fluorescence accounts for the instrument limited spike at short time.

At room temperature, the Gd phosphorescence decay (Figure 4) is a single exponential with a time constant of 22(2) μs at all emission wavelengths. No change in the lifetime was observed upon changing the laser intensity in the range from 5 to 200 mJ cm^{-2}. The optical density at 355 nm of a 100 nm thick evaporated film is 0.024, so the upper bound of this intensity range corresponds to an exciton density of 1.8×10^{20} cm^{-3}, which is comparable to the molecular density (7×10^{20} cm^{-3}). In other words, approximately 1 in 3 gadolinium complexes are simultaneously excited in the initial pulse. Lowering the temperature to 78 K increases the phosphorescence lifetime to 138(5) μs. The evolution of this lifetime with temperature is presented in Figure 5.

The bulk of the emission from Tb(tb-pmp)$_3$ is long-lived and emanates from the lanthanide ion. In addition to the intense metal-centered emission, however, Tb(tb-pmp)$_3$ presents a weak, spectrally broad, emission with 200(50) ns decay time (Figure 3). This band has a similar wavelength maximum and fwhm to the Gd(tb-pmp)$_3$ phosphorescence. Assuming that the ligand is effectively unperturbed by changes in the lanthanide ion, it is attributed to ligand-localized triplet emission. The emission spectrum of Tb(tb-pmp)$_3$ recorded with a 10 ns gate, delayed

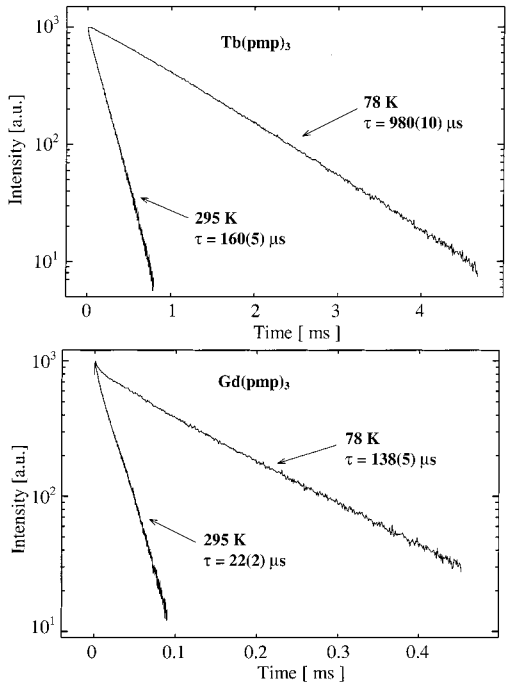

Figure 4. Microsecond kinetics. Luminescence decay at room temperature and 78 K of the terbium $^5D_4 \rightarrow {}^7F_5$ emission in Tb(tb-pmp)$_3$ detected at 18 300 cm^{-1} (excitation 28 170 cm^{-1}). Phosphorescence decay at room temperature and 78 K of Gd(tb-pmp)$_3$ detected at 19 200 cm^{-1} (excitation 28 170 cm^{-1}).

by 40 ns, indicates that the terbium emission is already dominant on the nanosecond time scale (Figure 6). Comparison with Figure 1, in which the spectrum was taken with a 500 μs delay, shows than the underlying spectrally broad phosphorescence is present at ~45 ns but absent at the later time. The inset in Figure 6 shows the time-evolution of the emission detected at different wavelengths, together with the location of the 40−50 ns gate used to obtain the spectrum. Curves a and c are recorded outside the range of the terbium emission bands. Each curve contains an initial peak of width ~10 ns, due to the convolution of the initial short-time (~20 ps) fluorescence pulse with the relatively slow instrument response function used for this set of measurements. In addition to this peak, a tail due to the ligand-localized phosphorescence is also present. Curve b comprises the fluorescence, phosphorescence and terbium emission. The change in going from a to c, in which both the phosphorescence and the fluorescence due to the ligand decrease, is a result of their spectral distribution (Figure 1). In the b curve, it is therefore safe to infer that the ligand-based emission is intermediate in intensity between a and c. Nevertheless, immediately after the initial fluorescence pulse, curve b has much more intensity than a and c. This indicates that the terbium already starts to emit at most a few nanoseconds after the excitation pulse. The time resolution allows us to estimate a rise time shorter than 10 ns for the majority of the terbium emission.

3.3. Lanthanide Emission. Figure 1 shows the Tb(tb-pmp)$_3$ lanthanide luminescence spectrum recorded in the period from 0.5 to 1.5 ms after the laser pulse. This emission is characteristic of the $^5D_4 \rightarrow {}^7F_J$ $f-f$ transitions (with $J = 6$, 5 and 4) of trivalent terbium ions.[19,20] All the $^5D_4 \rightarrow {}^7F_J$ emission lines of the terbium ion in the wavelength range 21 500−17 000 cm^{-1} show the same exponential decay with a 160(5) μs time constant at 295 K and 980(10) μs at 78 K (Figure 4). These decay times are independent of the exciton density, over the intensity range indicated in the previous section. The temperature dependence

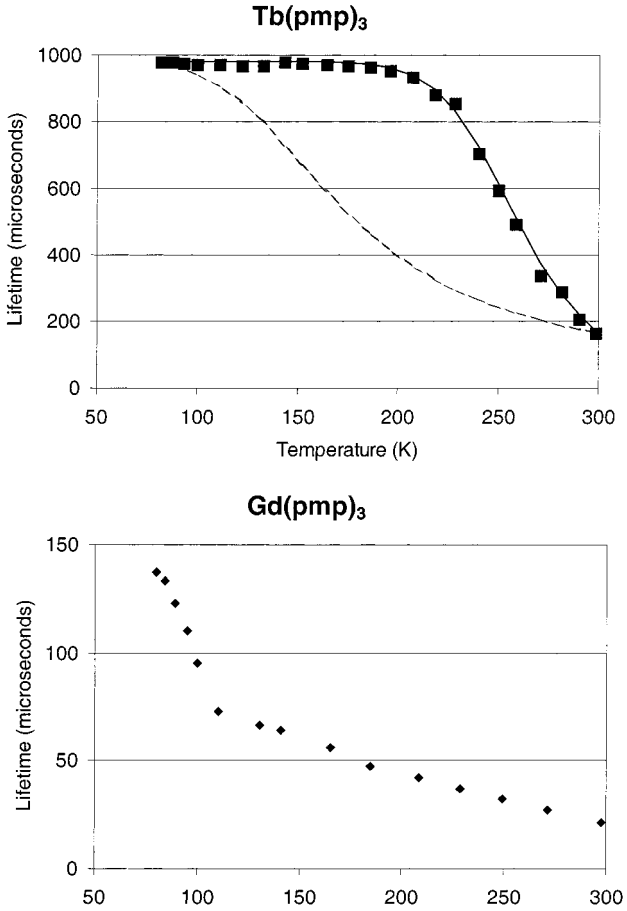

Figure 5. Temperature dependence of the luminescence lifetime in Tb(tb-pmp)$_3$ and Gd(tb-pmp)$_3$ (solid line has activation energy 2200 cm^{-1}, dashed line has activation energy 500 cm^{-1}).

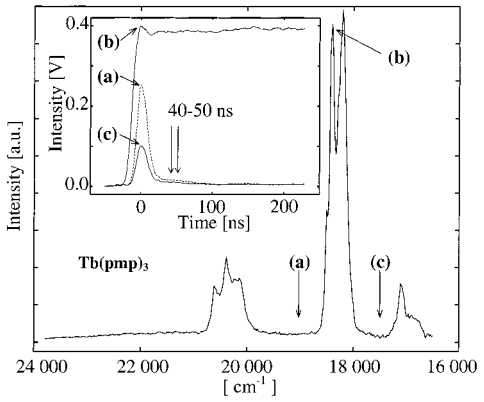

Figure 6. Emission spectrum of Tb(tb-pmp)$_3$ recorded with a 10 ns gate delayed by 40 ns (excitation 28 170 cm^{-1}, 295 K). The insert gives the nanosecond time-evolution of the emission detected at different wavelengths (a, b, and c) indicated by the corresponding arrows in the spectrum.

of this lifetime is presented in Figure 5. The 6-fold increase in the lifetime upon lowering the temperature is matched by an approximate 6-fold increase in the emission quantum yield. The quantum efficiency of the Tb emission has been measured[21] to be 12(1)% at 300 K, implying that the quantum yield for the metal-centered $f-f$ emission at 78 K is ~75%.

3.4. Mixed Materials. In solid solution samples containing Tb:Gd ratios of 1:99 or 5:95, the gadolinium phosphorescence and terbium f−f emission spectra are identical to those of the pure compounds shown in Figure 1. The relative intensities of these contributions are determined only by the composition of

the mixture. The results for powders in which the components were mechanically mixed were indistinguishable from those of the solid solutions. In every case, the lifetime of the component emissions is unchanged with respect to that found in the pure materials.

The total Gd and Tb emission intensities in the solid solutions, integrated over wavelength, are approximately equal at a Gd:Tb ratio of 100:1. Because the average emission wavelengths, and thus detection efficiencies, are not very different, the phosphorescence quantum yield for Gd(tb-pmp)$_3$ at room temperature is approximately one hundred times smaller than that of Tb(tb-pmp)$_3$ *f*−*f* emission at the same temperature, i.e., ∼0.1%.

4. Discussion

4.1. Ligand Energy Levels. We make the assumption that the ligand energy level schemes in Gd(tb-pmp)$_3$ and Tb(tb-pmp)$_3$ are similar. This is justified by Figure 1, which shows the close similarity between the fluorescence spectra of the two compounds. On the basis of the lifetime data, it is natural to assign the fluorescence to a ligand-centered singlet excited state and the phosphorescence to a triplet state. We make no further comment on the nature of these states, other than to note that there is sufficient absorption intensity in the region near 28 000 cm^{-1} ($\epsilon \approx 2000$ mol dm^{-3} cm^{-1}) where the pump laser photons are absorbed, to justify the presence of a spin-allowed intraligand transition, whereas there is no detectable absorption near 25 000 cm^{-1} in the region where the absorption that corresponds to the phosphorescence spectrum would be expected.

We distinguish these states for practical purposes by the labels S_1 and T_1. However, the total spin quantum number for the complex $S = 3$ for the ligand singlet states and 2 or 4 for the triplet states. Of these only the triplet with $S = 2$ carries the same nominal spin as the $^5D_4$ state on the terbium ion. However, because the ligand−metal interaction is very weak, the ligand and metal systems are treated as uncoupled. Assuming that the Stokes-shifts of the singlet (S_1) and triplet (T_1) excited states are similar, the energy difference between these two levels corresponds to the difference between the maxima of their emission. This gives a separation of ∼1800 cm^{-1} between the S_1 and T_1 levels of the ligand.

From Figure 1, the positions of the electronic origins of the singlet and Gd-triplet states can only be estimated approximately. Due to vibronic coupling, the emission bands are broadened on the low energy side of the electronic origins, whereas at room-temperature, some hot-band structure contributes intensity on the high energy side. We therefore locate the origins at around 22 800 and 21 000 cm^{-1} respectively.

In Figure 1, the emission centered near 20 500 cm^{-1} corresponds to transitions from $^5D_4$ multiplet to the $^7F_6$ ground state multiplet. Both are split by the ligand field into a manifold of states, typically spanning 200−400 cm^{-1}. The set of weak $^7F_6 \rightarrow {}^5D_4$ transitions in absorption must therefore be located close to, or somewhat above, 20 500 cm^{-1}. The relevant excited-state energies in Tb(tb-pmp)$_3$ thus consist of the Tb $^5D_4$ multiplet levels (centered at 20 500 cm^{-1}), with the T_1 state of the ligand ∼500 cm^{-1} above them, and the S_1 state in turn 1800 cm^{-1} above the triplet. (We return to this estimate in the section on emission quenching below). Figure 1 also indicates that the spectral overlap between both the S_1 and the T_1 emission spectra and the $^7F_6 \rightarrow {}^5D_4$ absorption spectrum are large, and occur at near-optimal wavelengths for energy transfer by the coupled-dipole mechanism.[22,23] The energies of the states and a summary of the characteristic times for transfer between them, as discussed below, are summarized in Figure 7.

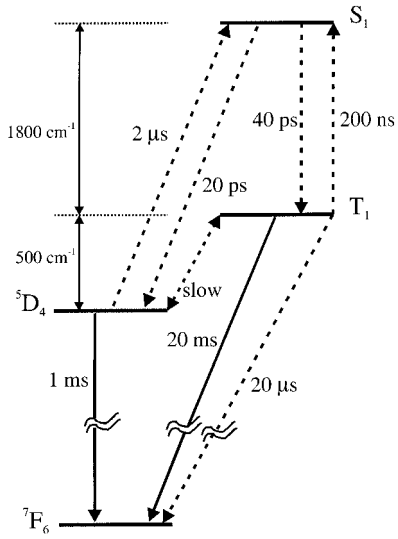

Figure 7. Postulated energy level and kinetic scheme for Tb(tb-pmp)$_3$

4.2. Intramolecular Dynamics. Because the S_1 lifetime is a factor of 2 shorter in the terbium complex, we propose that a second pathway exists that can also depopulate this level. The ligand ISC rate in Tb(tb-pmp)$_3$ is unlikely to differ markedly from that in Gd(tb-pmp)$_3$. The apparent lifetime of the T_1 state in Tb(tb-pmp)$_3$ is ∼200 ns, although this emission is weak. However, the rise-time of the majority of the terbium $^5D_4$ emission occurs in less than 10 ns, so the $S_1 \rightarrow T_1 \rightarrow Tb^{3+}$ energy-transfer mechanism, as usually postulated,[16] cannot be the principal pathway by which the $^5D_4$ levels are populated.

The simplest available additional path for S_1 decay consists of direct excitation transfer to the terbium ion. Such a mechanism has been proposed for some Eu^{3+} and Tb^{3+} complexes.[24−26] In Tb(tb-pmp)$_3$, the fluorescence spectrum extends from 23 000 to 18 000 cm^{-1} and thus covers an energy range that permits resonant excitation of the $^7F_6 \rightarrow {}^5D_4$ (at ∼20 500 cm^{-1}) transition of Tb^{3+}. Although it ought to be possible to observe the ∼20 ps rise time of the metal emission directly, equipment with a low enough repetition-rate to allow for relaxation of the $^5D_4$ population between measurements(i.e., <100 Hz), was not available to us. Nevertheless, we consider the effectively instantaneous appearance of terbium emission on the nanosecond time scale to be good evidence that the bulk of the singlet state population is transferred directly to the metal, rather than via the intermediate population of the ligand triplet manifold.

In view of the ionic nature of the metal−ligand bonding, the efficient screening of the *f*-orbitals from the ligand environment, and the fact that the ligand excitations have π-orbital character and thus negligible overlap with the metal, an exchange-coupled mechanism does not appear plausible in these compounds. Instead we follow Malta et al.,[27] in assuming that a coupled transition-multipole mechanism[22,23] is applicable. The energy transfer rate should then be proportional to the product of the integrated transition probabilities on both the donor and acceptor centers, modified by the integral of the joint density of states at the two centers. The latter can be related to the spectral overlap between the emission and absorption spectrum. Malta et al.[27] have pointed out that, using this model, the large transition moments expected for ligand singlet excitations predict rapid L→M (S_1→Tb) transfer.

From Figure 1, we note that the spectral overlaps of the $^7F_6 \rightarrow {}^5D_4$ transitions of Tb^{3+}near 20 500 cm^{-1} with the ligand singlet and triplet emission spectra are approximately equal, and in both cases large. The coupled transition dipole model then

predicts that the relative energy transfer rates from the singlet and triplet states should be approximately equal to the inverse ratio of the S_1 and T_1 radiative lifetimes. The former we can estimate from the oscillator strength in the region of the singlet absorption. Depending on what portion of the absorption spectrum is attributable to the S_1 state, its radiative lifetime could lie in the range 5−200 ns. The lower bound assumes that the relevant oscillator strength is that associated with the very strong $\pi \rightarrow \pi^*$ absorption, whose maximum is near 35 000 cm^{-1}. However, given that the fwhm of the S_1 emission is ∼3000 cm^{-1}, the S_1 absorption maximum would be expected to occur near 27 000 cm^{-1}, so this choice appears unrealistic. The upperbound for the S_1 lifetime is obtained by using the measured intensity near 27 000 cm^{-1}, and the fwhm of the fluorescence, to estimate the oscillator strength of a relatively weak singlet absorption centered at that energy. The S_1 radiative lifetime is unlikely to exceed 200 ns.

The radiative lifetime of the triplet state can be estimated from the quantum yield of the Gd(tb-pmp)$_3$ phosphorescence (∼0.1%) at room temperature, and the corresponding lifetime (∼20 μs), to be ∼20 milliseconds. On the basis of this simple argument, we would predict that the $S_1 \rightarrow$Tb rate could exceed the $T_1 \rightarrow$Tb transfer rate by a factor greater than 10^5. Whether the triplet state is an important intermediary, however, is determined by the relative rates of the $S_1 \rightarrow$Tb energy transfer and the $S_1 \rightarrow T_1$ intersystem crossing or initial branching ratio for the singlet excitation.

We conclude that both the $S_1 \rightarrow T_1$ intersystem crossing and the ligand-to-metal $S_1 \rightarrow$Tb transfer are very rapid in this system, taking place on a time scale of tens of picoseconds. In principle then, excitation transfer to Tb can occur from both the singlet and triplet states.

A comparison with the observations of Ying et al.,[28] who made measurements on Tb(tb-pmp)$_3$·2H$_2$O, is instructive. Their complexes are similar to those studied here with the exception of the two H$_2$O ligands. Despite the similarity of the materials, our measurement of the fluorescence lifetime (∼20 ps) contrasts with their result of 0.5 ± 0.3 ns. However, the measurements of Ying et al. are not self-consistent. If the measured fluorescence lifetime is taken as ∼1 ns, and the intrinsic radiative lifetime, taken from the absorption transition probability is ∼200 ns, the fluorescence quantum efficiency should be high. When viewed through the 10 ns gate, coincident in time with the excitation pulse, as used by these workers, any such fluorescence would completely swamp any metal emission which, with a radiative lifetime ∼1ms, has an oscillator strength ∼10^4 times weaker. In practice however, the spectrum taken under these conditions contains ligand fluorescence and terbium spectral features of comparable magnitude. Because the reported singlet lifetime is obtained by deconvolution from a 6 ns laser pulse profile, and the authors indicate that they cannot deconvolute lifetimes of less than 0.5 ns, the value they report lies at the limit of their method. We therefore believe that the singlet lifetime of Tb(tb-pmp)$_3$·2H$_2$O is more likely to be similar to those determined in this work.

4.3. Intermolecular Dynamics. No change of the phosphorescence lifetime in Gd(tb-pmp)$_3$ is observed as a function of the emission wavelength, indicating that the emission stems from a homogeneous set of emitting centers. Nor is any change seen as a function of laser power; there is thus no evidence for triplet−triplet annihilation, even at exciton densities of 1.8 × 10^{20} cm^{-3} that approach the molecular density. No change is observed in the Gd phosphorescence lifetime in a solid solution containing 1% or 5% Tb. Nor is there any detectable difference between mechanically mixed solids samples and solid solutions with the same composition, despite that fact that the typical migration distance of a triplet exciton to a terbium site could be 1 micron in the former case and 1 nm in the latter. In other words there is no evidence of triplet exciton migration between Gd(tb-pmp)$_3$ molecules and subsequent trapping by Tb(tb-pmp)$_3$ molecules. This is perhaps surprising as triplet−triplet energy transfer is a common phenomenon in organic crystals, and has been cited as an important loss process in some phosophorescent OLEDs.[29] The large Stokes shift for the triplet may well make this intermolecular energy transfer process unfavorable; energetic and coupling disorder in amorphous materials may also contribute.

There is also no change in the Tb emission lifetimes as a function of wavelength or laser power in the 1% Tb material—Thus, we observe no evidence for quenching processes, such as the migration of metal-centered excitations to trap sites or up-conversion. This is perhaps less surprising as the Ln ions are separated by more than 9 Angstrom, and the coupled-dipole transfer rate scales as R^{-6}. From a device point of view, the absence of significant excitation mobility on the time scale of the luminescence lifetime is advantageous. It both prevents the trapping of excitations at defect sites and eliminates losses from bi-exciton annihilation.

4.4. Emission Quenching. Despite the absence of significant intermolecular excitation transfer, the quantum efficiency of Tb emission at 78 K is 5−6 times greater than that at 300 K (Figure 5). Apparently then, a thermally activated intramolecular process reduces the quantum efficiency of the terbium luminescence at room temperature.

In what follows, the characteristic radiative and nonradiative times for inter-state dynamics are summarized in Figure 7. We shall assume the following electronic degeneracies: for the Tb $^5D_4$ manifold $(2J + 1) = 9$, for the three ligand triplets, $3 \times (2S + 1) = 9$, and for the three ligand singlets, $3 \times (2S + 1) = 3$. The best-fit activation energy for the temperature dependence of the Tb-lifetime data in Figure 5 is 2200 ± 200 cm^{-1} (shown as a solid line). This corresponds fairly closely to the energy gap to the S_1 state, and we therefore conclude that the thermally activated loss of population from $^5D_4$ occurs via this state.

If $^5D_4$ and S_1 were the only relevant states, the preexponential factor for this activated process would imply a loss of population from the S_1 state with a characteristic time of ∼5 ns. Although this approximates the estimated radiative lifetimes of S_1, the absence of measurable delayed fluorescence makes this hypothesis implausible. In addition, nonradiative losses from S_1 do not appear to be significant on the 20 μs time scale, otherwise they would be apparent as a ∼1700 cm^{-1} activated quenching of the T_1 emission in the gadolinium compound. Figure 5 shows that there is only a weak temperature dependence of the Gd phosphorescence between 100 and 300 K, so the S_1 state cannot be a source of fast nonradiative loss from the 3-level Tb system. (We do not know the reason for the strong temperature dependence of this lifetime below 100 K, but there may be a small exciton splitting of the three ligand triplet states.)

Given the efficiency of intersystem crossing, the most plausible route for rapid population loss from the three-level excited-state system in Tb(tb-pmp)$_3$ is via the triplet state. We assume the triplet lifetime is comparable to that measured for gadolinium (∼20 μs) and that its decay is dominated by nonradiative processes, as indicated by the low quantum efficiency (∼0.1%) of the T_1 emission in Gd(tb-pmp)$_3$. The triplet state is therefore the only plausible source of thermally

activated population loss from the 3-level system on a time scale short compared with rate of terbium emission (1 ms).

The simplest model for this loss is *direct* $^5D_4 \rightarrow T_1$ transfer. However, we will now argue that this process is too slow to be significant. First, we notice from the inset in Figure 6 and from Figure 3, that nearly all the population of the $^5D_4$ level is established within 10 ns of the excitation pulse. It follows that if a significant population is established in the T_1 level following rapid ISC, its transfer to $^5D_4$ must either be slow on the 200 μs time scale (because there is no significant rise time in Figure 3) or occur in less than 10 ns. In fact, a shorter limit than 10 ns can be set because the luminescence background in Figure 2 is almost constant on the time scale between 1 and 10 ns. This emission is detected at 21 300 cm^{-1} where the T_1 phosphorescence should dominate (Figure 1), and no significant change in the T_1 population due to transfer to $^5D_4$ is apparent within this period.

Because the energy gap between $^5D_4 \rightarrow T_1$ is $\sim$500 cm^{-1}, if the $T_1 \rightarrow$Tb transfer occurs in less than 10 ns, the time for $^5D_4 \rightarrow T_1$ back-transfer at room temperature would have to be less than $\sim$100 ns. This rate is fast compared to the decay of both $^5D_4$ and T_1, so equilibrium should be rapidly established between them. It is then possible to simulate the temperature dependence of the lifetime of the $^5D_4$ population in Figure 5 (dashed line), using an energy difference of 500 cm^{-1}, together with a 20 μs T_1 decay time. The result, however, is in markedly poor agreement with the data. We are therefore forced to conclude that at room temperature *direct* thermally activated $^5D_4 \rightarrow T_1$ transfer occurs slowly on the 100 μs time scale.

On the other hand, this transfer can also occur *indirectly* via the S_1 state, with an appropriate $\sim$2300 cm^{-1} activation energy (Figure 7). Because the $S_1 \rightarrow {}^5D_4$ transfer has a characteristic time of $\sim$20 ps at room temperature, we can deduce that the time for the back-transfer, at the same temperature, is $\sim$2 μs. Because the $S_1 \rightarrow T_1$ ISC time is short ($\sim$40 ps) on this time scale, the $^5D_4 \rightarrow S_1$ back-transfer rate determines the rate of *indirect* $^5D_4 \rightarrow T_1$ back-transfer. If the decay of the triplet state occurs in a time comparable to that in the gadolinum compound ($\sim$20 μs), the $^5D_4$ and T_1 state populations should be close to those that would be predicted were they at equilibrium. At low temperatures (<200 K), however, the $^5D_4 \rightarrow S_1$ back-transfer rate becomes comparable to or slower than the 1 ms radiative decay rate from $^5D_4$, so that indirect transfer to T_1 no longer provides a significant depopulation mechanism.

The assumption of near-equilibrium between $^5D_4$ and T_1 is consistent with the observed lifetime of the Tb emission at room temperature, since an energy difference of 500 cm^{-1} leads to a $^5D_4$:T_1 population ratio of $\sim$10:1. Assuming the $^5D_4$ lifetime to be 1 ms (i.e., the same as its low-temperature value), and that of T_1 to be the same as the 20 μs measured in the gadolinium sample (i.e., 50 times shorter), we can indeed account for the 5-fold reduction in the $^5D_4$ emission lifetime and quantum yield (illustrated in Figure 5), because at equilibrium $\sim$10% of the population is present in the T_1 state. Note that, because of its low quantum yield, the triplet phosphorescence associated with the near-equilibrium T_1 population is expected to be undetectably weaker ($\sim 10^{-4}$) than the $^5D_4$ emission.

Within this framework it is possible to rationalize processes that occur on the 10 ns to 1 μs time scale. A fit to the transient emission near 19 200 cm^{-1} (Figure 3) indicates that, at room temperature, the broad underlying T_1 phosphoresence decays with a characteristic time of 200(50) ns. At the same time there is some evidence (Figure 6, curve (b)) of a small ($\sim$5%) rise in the $^5D_4$ emission on the same time scale. Following the initial population of the S_1 state, our TCSPC results show that the $S_1 \rightarrow {}^5D_4$ and ISC transfers both occur within $\sim$40ps. The branching ratio in Tb(tb-pmp)$_3$ between these two routes cannot be determined with precision, because we can only guess the rate of ISC in the Tb-compound by comparing its rate in the Gd-compound. Branching is, however, unlikely to lead to instantaneous $^5D_4$ and T_1 populations that are in thermal equilibrium. If, for example, the transient population of T_1 is greater than 10% of the total, equilibrium would be subsequently established most rapidly by indirect transfer through S_1. The rate of this process can be estimated by assuming, from the Gd fluorescence data, that the ISC $S_1 \rightarrow T_1$ decay time is $\sim$40 ps. If the $S_1 - T_1$ separation is taken as $\sim$1800 cm^{-1} the characteristic time for $T_1 \rightarrow S_1$ back-transfer is $\sim$400 ns, in reasonable agreement with the evidence for a $\sim$200 ns decay in the T_1 phosphorescence. At low temperatures there can be no activated back-transfer from T_1 via the singlet state to $^5D_4$, so the high ($\sim$75%) quantum yield of metal emission indicates that a high proportion of the S_1 population is successfully transferred to the metal. On the other hand, at room temperature the instantaneous T_1 population is greater than the equilibrium value of 10%. Judging by the $\sim$5% increase in the metal emission on the 200 ns time scale the initial T_1 population represents $\sim$15% of the total. If it is assumed that the S_1 branching ratio is independent of temperature we can estimate the relative rates of transfer to $^5D_4$ compared to T_1 as $\sim$4:1.

Finally we consider whether the absence of direct $T_1 \rightarrow {}^5D_4$ transfer on a time scale short compared to 20 μs is plausible. If, as assumed here and by others[27] the coupled transition-multipole mechanism is valid, the relative magnitudes of the S_1 and T_1 radiative lifetimes, should largely determine the relative rates of $S_1 \rightarrow {}^5D_4$ and $T_1 \rightarrow {}^5D_4$ transfer. Using the estimated radiative lifetimes, the $S_1 \rightarrow {}^5D_4$ rate should exceed the $T_1 \rightarrow {}^5D_4$ rate by a factor of $\sim 10^5 - 10^6$. If the ISC rate is approximately equal to the former, as we observe experimentally, then the back-ISC rate, for a $T_1 - S_1$ energy gap of $\sim$1800 cm^{-1} ($\sim$9kT), will be $\sim 2 \times 10^4$ times slower than the forward process, but still faster than the direct $T_1 \rightarrow {}^5D_4$ rate by one or 2 orders of magnitude based on the predictions of the coupled-dipole model. In other words, the activated process via the singlet state is indeed predicted, on the basis of this inevitably crude model, to be substantially faster than the direct transfer.

We conclude that nonradiative decay from the triplet manifold limits the efficiency of terbium luminescence. It appears, therefore, that a luminescence efficiency increase by a factor of $\sim$5, in a room-temperature device, could be obtained by using a redesigned ligand in which the energies of the ligand states are raised by $\sim$1000 cm^{-1} relative to the terbium levels. Because the triplet state has a long radiative lifetime, most of its population can be lost nonradiatively on the 20 μs time scale. In view of the slow rate of direct $T_1 \rightarrow {}^5D_4$ transfer we anticipate that, in any alternative ligand system, a high quantum efficiency will only be possible if a back-transfer pathway via a singlet state exists, with a similar activation energy to that found here, that enables energy transfer to the metal to compete with the triplet losses.

5. Conclusions

The observations above have a number of important implications for the design of OLED devices. The choice of a ligand like (tb-pmp) which has singlet and triplet states of similar energy which are both strongly vibrationally coupled, and have large emissive Stokes shifts and good spectral overlap with absorptive metal states, in principle, allows efficient ligand-to-

metal energy transfer that can occur during the lifetimes of both the triplet *and* the singlet states. In particular, the very rapid S_1 ligand-to-metal energy transfer competes effectively with ligand intersystem crossing, and also with other singlet emission radiative and nonradiative quenching processes. All such alternative pathways that deactivate the singlet state potentially lead to device losses if, as is the case here, nonradiative losses from the triplet state occur more rapidly than energy transfer to the metal.

The quantum yield and lifetime measurements as a function of temperature imply that there is the potential for an increase in device efficiency by a factor of about 6. We have, however, observed no evidence for triplet−triplet energy migration, nor for Tb−Tb energy transfer in these materials, even at very high exciton densities. Both these processes are potential mechanisms for decreasing the quantum yield in electroluminescent devices.

This result is striking because it has been argued that, in electroluminescent devices, triplet−triplet (bi-exciton) annilation may be a general mechanism limiting the current density (J_0), and therefore brightness, at which the device efficiency begins to roll-off.[30] In this model $J_0 \propto 1/\tau^2$ where τ is the lifetime of the luminescent state. If this is correct, compounds with short triplet radiative lifetimes, such as transition metal compounds in which the spin selection rule is relaxed by the spin−orbit interaction, should be preferred for high brightness displays. Apparently though, this mechanism does not apply in the compounds studied here, because they maintain high photoluminescence quantum efficiencies at high exciton densities, despite possessing long emissive lifetimes. Nevertheless, the efficiencies of Tb(tb-pmp)$_3$ OLEDs do roll-off at high current densities,[13] so an alternative quenching process must operate. We assume that this is polaron-exciton annihilation, which can lead to the same current density dependence of the electroluminescence quantum efficiency as biexciton annihilation, providing that the current is space-charge limited.[30] Simply put, the excited-state responsible for the emission is deactivated not by interactions with another excited molecule, but with a neighboring charge carrier. In Tb(tb-pmp)$_3$ electroluminescent devices, the most mobile carriers are ligand-based holes, so exciton−polaron annihilation could be viewed as the transfer of an f-electron from an excited [Tb(III)(tb-pmp)$_3$]* molecule to a ligand-based hole on an adjacent molecule. The resultant [Tb(IV)(tb-pmp)$_3$]$^+$ species would then relax to a Tb(III) configuration with a hole on a ligand.

Finally, we note that the rapid ISC in this ligand system means that there should be no loss of electroluminescence efficiency due to the spin state of the excitons formed on electron−hole recombination. However, if population is trapped in ligand triplet states, slow energy transfer to the lanthanide could cause a major loss of quantum efficiency. Whether this will happen depends on the details of the electronic structure of the ligand.

Acknowledgment. We thank Stan Botchway and Mike Towrie of Rutherford Appleton Laboratories for their help with TCSPC measurements, as well as the EPSRC for access to Mass Spectrometry facilities. J.M.R. thanks the Swiss National Science Foundation for financial support. V.C, S.E.W and M.G were supported by Opsys Ltd.

References and Notes

(1) Tsutui, T. *MRS Bulletin* **1997**, *22*, 39
(2) Kido, J.; Hayase, H.; Hongawa, K.; Nagai K.; Okuyama, K. *Appl. Phys. Lett.* **1994**, *65*, 2121.
(3) Wang, K. Z.; Li, L. J.; Liu, W. M.; Xue, Z. Q.; Huang, C. H.; Lin, J. H. *Mater. Res. Bull.* **1996,** *31*, 993.
(4) Zhang, X.; Sun, R.; Zheng, Q.; Kobayashi, T. *Appl. Phys. Lett.* **1997,** *71*, 2596.
(5) Kido, J.; Nagai, K.; Okamoto, Y. J. *J. Alloys Compd.* **1993**, *192*, 30.
(6) Li, W. L.; Yu, J. Q.; Sun, G.; Hong, Z. R.; Yu, Y.; Zhao, Y.; Peng, J. B.; Tsutui, T. *Synth. Met.* **1997**, *91*, 263.
(7) Christou, V.; Salata, O. V.; Tuan, Q. L.; Capecchi, S.; Bailey, N. J.; Cowley, A.; Chippindale, A. M. *Synthetic Metals* **2000**, *111−112*, 7.
(8) Bell, J. *Opto & Laser Europe* **1999**, *60*, 21.
(9) Holz, R. C.; Thompson, L. C. *Inorg. Chem.* **1993**, *32*, 5251.
(10) Malta, O. L.; Brito, H. F.; Menezes, J. F. S.; Goncalves e Silva, F. R.; Alves, S., Jr.; Farias, F. S., Jr.; Andrade, A. V. M. D. *J. Lumin.* **1997**, *75*, 255.
(11) Gao, X. C.; Cao, H.; Huang, C. H. *Appl. Phys. Lett.* **1998**, *72*, 2217.
(12) Liang, C. J.; Li, W. L. *Synth. Met.* **1997**, *91*, 151.
(13) Capecchi, S.; Renault, O.; Moon, D. G.; Halim, M.; Etchells, M.; Dobson, P. J.; Salata, O. V.; Christou, V. *Adv. Mater.* **2000**, *12*, 1591.
(14) Cotton, S. *Lanthanides and Actinides*; Oxford University Press: New York, 1991.
(15) Shannon, R. D. *Acta Crystallogr.* **1976**, *A32*, 751.
(16) Buono-Core, G. E.; Li, H.; Marciniak, B. *Coord. Chem. Rev.* **1990,** *99*, 55.
(17) Jensen, B. S. *Acta Chem Scand.* **1959**, *13*, 1668.
(18) Christou, V. et al. in preparation.
(19) Diecke, G. H. *Spectra and Energy Levels of Rare Earth Ions in Crystals*; John Wiley and Sons: New York, 1968.
(20) Wybourne, B. G. *Spectroscopic Properties of Rare Earths*; John Wiley and Sons: New York, 1965.
(21) Measurement by Prof. Ifor Samuel and Dong Ma, University of St Andrews with excitation at 30 800 cm^{-1}.
(22) Forster, T. *Ann. Phys (Paris)* **1948**, *2*, 55.
(23) Dexter, D. L. *J. Chem. Phys.* **1953**, *21*, 836.
(24) Crosby, G. A. *Mol. Cryst.* **1966**, *1*, 37.
(25) Horrocks, W. W.; Albin, M. *Prog. Inorg. Chem.* **1984**, *31*, 9.
(26) Alaoui, I. M. *J. Phys. Chem.* **1995**, *99*, 13 280.
(27) Malta, O. L. *J. Lumin.* **1997**, *71*, 229.
(28) Ying, L.; Yu, A.; Zhao, X.; Li, Q.; Zhou, D.; Huang, C.; Umetani, S.; Matasai, M. *J. Phys. Chem.* **1996**, *100*, 18 387.
(29) Kwong, R. C.; Sibley, S.; Dubovoy, T.; Baldo, M.; Forrest, S. R.; Thompson, M. E. *Chem. Mater.* **1999**, *11*, 3709.
(30) Baldo, M. A.; Adachi, C.; Forrest, S. R. *Phys. Rev. B* **2000,** *62*, 10 967.